J|A|C|S
ARTICLES
Published on Web 11/05/2002

Structural Dependencies of $^{h3}J_{NC'}$ Scalar Coupling in Protein H-Bond Chains

Nenad Juranić,*,† Martin C. Moncrieffe,‡ Vladimir A. Likić,§ Franklyn G. Prendergast,† and Slobodan Macura†

Contribution from the Department of Biochemistry and Molecular Biology, Mayo Graduate School, Mayo Clinic and Foundation, Rochester, Minnesota 55905, Department of Biochemistry, University of Cambridge, Cambridge CB2 IGA, England, and Department of Biochemistry, University of Melbourne, Melbourne, Australia

Received June 17, 2002

Abstract: The H-bond ($^{h3}J_{NC'}$) and peptide bond ($^{1}J_{NC'}$) scalar couplings establish connectivity of the electronic structure in the H-bond chains of proteins. The correlated changes of $^{h3}J_{NC'}$ and $^{1}J_{NC'}$ couplings extend over several peptide groups in the chains. Consequently, the electronic structure of the H-bond chains can affect $^{h3}J_{NC'}$ in a manner that is independent of the local H-bond geometry. By taking this into account, and by using a more complete set of H-bond geometry parameters, we have predicted $^{h3}J_{NC'}$ couplings in the H-bond chains with deviations commensurate to the standard deviations of the experimentally determined values. We have created a comprehensive database of $^{h3}J_{NC'}$ and $^{1}J_{NC'}$ couplings by measuring the coupling constants in ubiquitin ($\alpha\beta$-fold) intestinal fatty acid binding protein (β-barrel) and carp parvalbumin (α-helical).

Introduction

Before the discovery of nuclear scalar couplings across hydrogen bonds (H-bonds) in proteins[1,2] their existence in proteins in solution was usually inferred rather than actually observed. The direct observation of H-bond $^{h3}J_{NC'}$ couplings provided a powerful tool for furthering the structural characterization of proteins. The magnitude of the $^{h3}J_{NC'}$ scalar coupling depends on the H-bond geometry,[3−7] which has been utilized in several studies of H-bonds in proteins.[8−12]

The structural dependencies of the $^{h3}J_{NC'}$ scalar couplings have been successfully interpreted in the immunoglobulin binding domain of protein G.[3,4] For human ubiquitin, in which $^{h3}J_{NC'}$ were first observed,[1,2] structural correlations were poor. This has been ascribed to insufficient resolution (1.8 Å) of the X-ray crystal structure.[13] However, molecular dynamics simulations (MD) have shown that protein flexibility broadens the distribution of H-bond geometry parameters,[14] and thus the resolution obtained by X-ray diffraction may not be the actual source of error. An altered structure of the protein in solution relative to that seen crystallographically is improbable, because the NMR solution structure of human ubiquitin[15] is very similar to that derived from X-ray crystallographic analysis.

Recently,[16] H-bond chains in the H-bonding network of protein were characterized by the continuous sequence of H-bond ($^{h3}J_{NC'}$) and peptide bond ($^{1}J_{NC'}$) scalar couplings: $-{}^{1}J_{NC'}-{}^{h3}J_{NC'}-{}^{1}J_{NC'}-$. The observed correlation between $^{h3}J_{NC'}$ and $^{1}J_{NC'}$ couplings in these chains indicates that variations in the peptide bond electronic structure could affect $^{h3}J_{NC'}$ independent of the local H-bond geometry. The present work investigates the importance of this effect. To expand the database we have determined $^{h3}J_{NC'}$ and $^{1}J_{NC'}$ couplings in two additional proteins with differing folds: the β-barrel intestinal fatty acid binding protein (apo-IFABP)[17] and the α-helical carp parvalbumin in the calcium saturated state (holo-CPV).[18] The solution NMR derived structures of both proteins agree with the crystal structures,[19,20] except for some local differences in apo-IFABP.

† Mayo Clinic and Foundation.
‡ University of Cambridge.
§ University of Melbourne.

(1) Cordier, F.; Grzesiek, S. *J. Am. Chem. Soc.* **1999**, *121*, 1601−1602.
(2) Cornilescu, G.; Hu, J.-S.; Bax, A. *J. Am. Chem. Soc.* **1999**, *121*, 2949−2950.
(3) Cornilescu, G.; Ramirez, B. E.; Frank, M. K.; Clore, G. M.; Gronenborn, A. M.; Bax, A. *J. Am. Chem. Soc.* **1999**, *121*, 6275−6279.
(4) Barfield, M., *J. Am. Chem. Soc.* **2002**, *124*, 4158−4169.
(5) Bagno, A. *Chem. Eur. J.* **2000**, *6*, 2925−2930.
(6) Adalsteinsson, A.; Maulitz, H.; Bruice, C. T. *J. Am. Chem. Soc.* **1996**, *118*, 7689−7693.
(7) Scheurer, C.; Bruschweiler, R. *J. Am. Chem. Soc.* **1999**, *121*, 8661−8662.
(8) Li, H.; Yamada, H.; Akasaka, K.; Gronenborn, A. M. *J. Biomol. NMR* **2000**, *18*, 207−216.
(9) Cordier, F.; Wang, C.; Grzesiek, S.; Nicholson, I. K. *J. Mol. Biol.* **2000**, *304*, 739−752.
(10) Jaravine, V. A.; Alexandrescu, A. T.; Grzesiek, S. *Protein Sci.* **2001**, *10*, 943−950.
(11) Alexandrescu, A. T.; Snyder, D. R.; Abildgaard, F. *Protein Sci.* **2001**, *10*, 1856−1868.
(12) Cordier, F.; Grzesiek, S. *J. Mol. Biol.* **2002**, *317*, 739−752.
(13) Vijay-Kumar, S.; Bugg, C. E.; Cook, W. J. *J. Mol. Biol.* **1987**, *194*, 531−544.
(14) Buck, M.; Karplus, M. *J. Phys. Chem.* **2001**, *105*, 11000−11015.
(15) (a) Cornilescu, G.; Marquardt, J. L.; Ottiger, M.; Bax, A. *J. Am. Chem. Soc.* **1998**, *120*, 6836−6837. (b) Babu, R. C.; Flynn, P. F.; Wand, A. J. *J. Am. Chem. Soc.* **2001**, *123*, 2691−2692.
(16) Juranić, N.; Macura, S. *J. Am. Chem. Soc.* **2001**, *123*, 4099−4100.
(17) Scapin, G.; Gordon, J. I.; Sacchettini, C. *J. Biol. Chem.* **1992**, *267*, 4253−4269.
(18) Kumar, V. D.; Lee, L.; Edwards, B. F. *Biochemistry* **1990**, *29*, 1404−1412.
(19) Moncrieffe, M. C.; Juranić, N.; Kemple, M. D.; Potter, J. D.; Macura, S.; Prendergast, F. G. *J. Mol. Biol.* **2000**, *297*, 147−163.
(20) Hodson, M. E.; Cistola, D. *Biochemistry* **1997**, *16*, 1450−1460.

Scheme 1

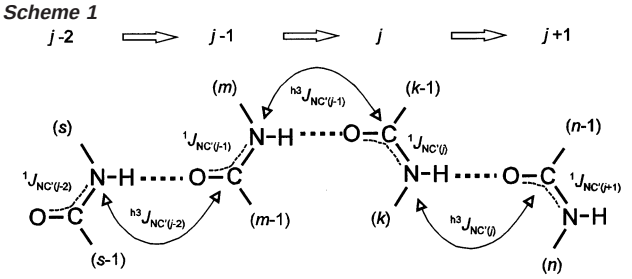

Results and Discussion

We have determined approximately 190 $^{h3}J_{NC'}$ and 300 $^{1}J_{NC'}$ coupling constants in the three proteins (ubiquitin, holo-CPV and apo-IFABP). These represent all $^{1}J_{NC'}$ couplings, and about 80% of the $^{h3}J_{NC'}$ couplings expected from the proteins X-ray crystal structures[13,17,18] (using a H-bond cutoff distance of 3.5 Å). Most of the missing data belong to H-bonds at position 4 in reverse turns. Approximately 10% of the determined $^{h3}J_{NC'}$ couplings represent H-bonds not expected from the crystal structures and these are predominantly H-bonds formed between peptide groups and side-chains.

Correlations between $^{h3}J_{NC'}$ and $^{1}J_{NC'}$ Couplings in the Chains of H-Bond Networks. It is remarkable that scalar couplings between the ^{15}N and ^{13}C nuclei of peptide groups establish connectivity of electronic structure in the protein H-bond chains. The H-bonding chain is detected by the sequence of the scalar couplings: $-{}^{1}J_{NC'(j-1)}-{}^{h3}J_{NC'(j-1)}-{}^{1}J_{NC'(j)}-{}^{h3}J_{NC'(j)}-{}^{1}J_{NC'(j+1)}-$ (Scheme 1).

The index $j + r$ ($r \in ..., -2, -1, 0, 1, 2, ...$) defines the relative position of a peptide group in the H-bond chain and increases in the direction of proton donation (the "downstream" direction). The same $^{h3}J_{NC'}$ can be annotated either by the protein sequential numbers ($^{h3}J_{NC'}(k,n-1)$)[16] or by the H-bond chain index of the proton donor peptide group ($^{h3}J_{NC'(j)}$). The later annotation is more convenient in the analysis of relationships between the scalar couplings in the chain.

Previously, we characterized chains of three peptide groups.[16] In this work, chains of H-bonds were detected in length up to eight peptide groups, with the majority of the longer chains being seen in the β-barrel of apo-IFABP. The chains are found much in accordance with the X-ray crystal structure H-bond networks. Several chains were shorter due to spectral overlap that prevented measurement of $^{h3}J_{NC'}$, but few were prolonged by new capping H-bonds of the residues side-chains. A good sampling of chains with four peptide groups was obtained (43 examples). As found previously,[16] the coupling constants are strongly correlated (Figure 1).

The $^{h3}J_{NC'}$ couplings exhibit positive slope of correlation with each other over the whole length of a chain; a feature that has been attributed to the cooperativity of H-bonds.[16] They are also correlated with a negative slope to the $^{1}J_{NC'}$ couplings. The strongest correlation is seen between $^{h3}J_{NC'(j)}$ and $^{1}J_{NC'(j)}$ couplings that share the same nitrogen, which was ascribed to competition for *s*-electron density on nitrogen.[16] Also, correlation of $^{h3}J_{NC'(j)}$ with the peptide bond coupling at the "upstream" position, $^{1}J_{NC'(j-1)}$, is significant, while correlation to "downstream" $^{1}J_{NC'(j+1)}$ is weak. This asymmetry, or directionality of the peptide groups' influence, may be explained by a mechanism of peptide group polarization.[16,21,22]

H-Bond Geometry and $^{h3}J_{NC'}$ Couplings. The analysis of the $^{h3}J_{NC'}$ dependence on H-bond geometry may be affected by the correlations between $^{h3}J_{NC'}$ and $^{1}J_{NC'}$ in H-bond chains. This would occur if a correlation exists between $^{h3}J_{NC'}$ and $^{1}J_{NC'}$ which is independent of the local H-bond geometry. For example, $^{h3}J_{NC'}$ is usually not observed in the H-bonds of reverse turns in the presence of the large competing $^{1}J_{NC'}$ (Figure 2), although the H-bond distances are favorable. Additionally, the $^{h3}J_{NC'(j)}$ couplings are significantly affected by $^{1}J_{NC'(j-1)}$, so that the H-bond chain of three peptide groups has to be considered. With this requirement and the exclusion of H-bond bifurcation we have found 91 data points from the three proteins (ubiquitin 21 entries, holo-CPV 24 entries and apo-IFABP 46).

The parameters for the H-bond geometry were taken from the respective X-ray crystal structures.[13,17,18] The definitions of the H-bond parameters used in this work are given in Figure 3.

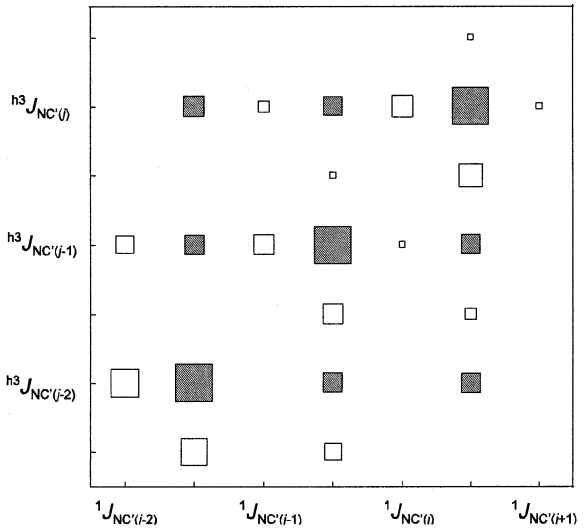

Figure 1. Correlation among $^{h3}J_{NC'}$ and $^{1}J_{NC'}$ couplings in selected (2.7 Å < d_{NO} < 3.2 Å) H-bond chains consisting of four peptide groups in ubiquitin, holo-CPV, and apo-IFABP. Correlation coefficients are represented by the area of squares ($^{h3}J_{NC'}$ vs $^{h3}J_{NC'}$, ■; $^{h3}J_{NC'}$ vs $^{1}J_{NC'}$, □), with the largest square having an r^2 of 0.4. Coefficients involving $^{1}J_{NC'}$ vs $^{1}J_{NC'}$ couplings are not displayed, for clarity.

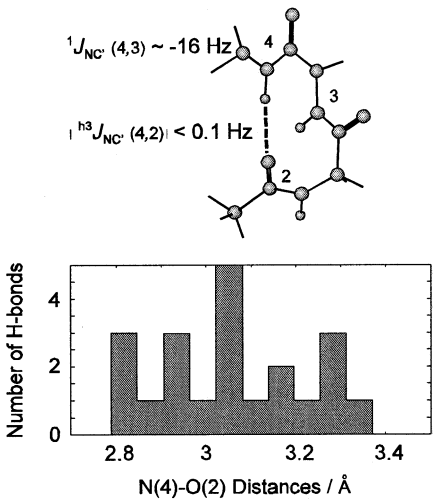

Figure 2. Examples of reverse turns from apo-IFABP, ubiquitin, and holo-CPV that have favorable H-bond distances but for which H-bond $^{h3}J_{NC'}$ couplings were not observed.

(21) Milner-White, E. J. *Protein Sci.* **1997**, *6*, 2477−2482.
(22) Juranić, N.; Ilich, P. K.; Macura, S. *J. Am. Chem. Soc.* **1995**, *117*, 405−410.

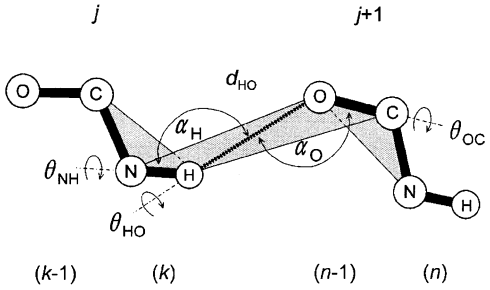

Figure 3. Six parameters of the peptide groups' position related to H-bonding: H-bond distance, d_{HO} ($H_k{}^j\cdots O_{n-1}{}^{j+1}$); H-bond angle at hydrogen, α_H ($N_k{}^j-H_k{}^j\cdots O_{n-1}{}^{j+1}$); H-bond angle at oxygen, α_O ($H_k{}^j\cdots O_{n-1}{}^{j+1}-C_{n-1}{}^{j+1}$); dihedral angle θ_{HO} between planes defined by atoms $N_k{}^j-H_k{}^j\cdots O_{n-1}{}^{j+1}$ and $H_k{}^j\cdots O_{n-1}{}^{j+1}-C_{n-1}{}^{j+1}$; dihedral angle θ_{NH} between planes defined by atoms $C_{k-1}{}^j-N_k{}^j-H_k{}^j$ and $N_k{}^j-H_k{}^j\cdots O_{n-1}{}^{j+1}$; dihedral angle θ_{OC} between planes defined by atoms $H_k{}^j\cdots O_{n-1}{}^{j+1}-C_{n-1}{}^{j+1}$ and $O_{n-1}{}^{j+1}-C_{n-1}{}^{j+1}-N_n{}^{j+1}$. A positive sign of a dihedral angle θ_{PQ} is associated with clockwise rotation when viewed along the P ⟹ Q direction.

The dependence of $^{h3}J_{NC'}$ on the H-bond geometry has been formulated as an exponential dependence on H-bond distance.[3] This was recently expanded to include the dependence on one H-bond angle and on one dihedral angle of the H-bonded peptide groups.[4] Application of this later equation (eq 14 in ref 4) to our data produced a correlation coefficient, r^2, of 0.644. However, adjustment of the coefficients in the same equation (eq 1) improved the r^2 value to 0.720 (Figure 4A).

$$^{h3}J_{NC'(j)} = [-0.74\cos^2\alpha_O + (-0.1\cos^2\theta_{OC} + 0.3\cos\theta_{OC} + 0.13)\sin^2\alpha_O]\exp[-2.7(d_{HO} - 1.76)] \quad (1)$$

Peptide Bond and $^{h3}J_{NC'}$ Couplings. The theoretical model of eq 1 does not consider structural variations of the peptide group. However, in peptide structures obtained to ultrahigh resolutions (~0.5 Å) the variations are visible (see Appendix). In general, the geometric changes of the peptide groups are too small for direct determination from the protein X-ray structures and consequently, some parameters of the peptide group geometry may be obtained with better precision indirectly. Thus the $^1J_{NC'}$ coupling constant is related to peptide-bond ($d_{NC'}$) length (Appendix), and the relative error of determination for $^1J_{NC'}$ in proteins is ~100 times smaller than for $d_{NC'}$. Also, the angle of pyramidalization at carbon is related to the protein backbone torsion angle Ψ_{k-1},[23] end the relative error for Ψ_{k-1} is ~10 times smaller. Both of these indirect parameters of the peptide group structure have strong correlation with $^{h3}J_{NC'}$. Most significantly, they correlate better with $^{h3}J_{NC'}$ than with the local H-bond geometry, which implies that they account for a separate dependence of $^{h3}J_{NC'}$ on the electronic structure of peptide groups. In Table 1 we present correlation coefficients among $^{h3}J_{NC'}$, functions of the H-bond geometry, and functions of the peptide group structure (for comparison we have included amide proton chemical shifts as a parameter whose correlation to $^{h3}J_{NC'}$ is derived from their common dependence on the local H-bond geometry). In the H-bond chains, a peptide group structure is affected by other peptide groups and $^{h3}J_{NC'(j)}$ correlates with better exclusivity to a composite value of the peptide bond couplings: $^1J_\Sigma = 0.50\,^1J_{NC'(j)} + 0.35\,^1J_{NC'(j-1)} + 0.15\,^1J_{NC'(j+1)}$.

A probable cause for the relationship between $^{h3}J_{NC'}$ and the peptide group parameters is sharing of the s-electron density on nitrogen among the peptide bond and the H-bond. Indeed, $^1J_{NC'}$ coupling is the most exclusive in the correlation with $^{h3}J_{NC'}$ coupling, and the two couplings oppose each other. The piramydalization at carbon also may have an effect on the s-electron density. Other parameters of the peptide group geometry that should be considered, such as twist angle and pyramidalization at nitrogen, are left out because of the low precision of their determination. A change of available s-electron density requires scaling of the H-bond geometry dependence, therefore eq 1 should be multiplied by a factor proportional to the $^{h3}J_{NC'}$ coupling. The factor was formulated based on the

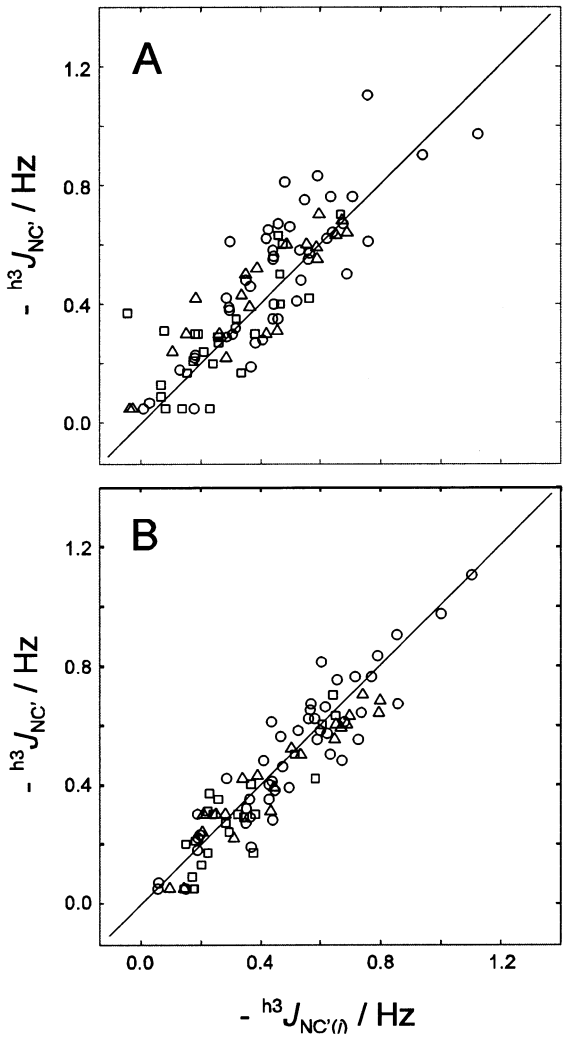

Figure 4. Correlation of $^{h3}J_{NC'}$ couplings with functions of the H-bond geometry: (△) human ubiquitin, (□) holo-CPV, (○) apo-IFABP. (A) Best fit ($r^2 = 0.722$) to the equation reported by Barfield,[4] here eq 1. (B) Best fit ($r^2 = 0.863$) to eq 2, which includes relation between $^{h3}J_{NC'}$ and $^1J_{NC'}$ couplings

Table 1. Correlation Coefficients (r^2) among Parameters

	$^{h3}J_{NC'(j)}{}^a$	eq 1	$^1J_{NC'(j)}$	$^1J_\Sigma{}^{c,d}$	sin $\Psi_{k-1}{}^c$	$\delta_{1H}{}^e$
$^{h3}J_{NC'(j)}{}^a$	1	0.72	0.21	0.32	0.32	0.48
eq 1^b	0.72	1	0.06	0.09	0.28	0.52
$^1J_{NC'(j)}$	0.21	0.06	1	0.59	0.05	0.04
$^1J_\Sigma{}^{c,d}$	0.32	0.09	0.59	1	0.03	0.08
sin $\Psi_{k-1}{}^c$	0.32	0.28	0.05	0.03	1	0.42
$\delta_{1H}{}^e$	0.48	0.52	0.04	0.08	0.42	1

[a] H-bond coupling constant. [b] H-bond geometry function. [c] Peptide group structure functions. [d] $^1J_\Sigma = 0.50\,^1J_{NC'(j)} + 0.35\,^1J_{NC'(j-1)} + 0.15\,^1J_{NC'(j+1)}$. [e] Amide proton chemical shift.

(23) Esposito, L.; Vitagliano, L.; Zagari, A.; Mazzarella, L. *Protein Sci.* **2000**, *9*, 2038−2043.

correlations in Table 1 and found to be $[15 + (0.27)\sin \Psi_{k-1} + (0.9)^1J_\Sigma]/3$. It approaches zero for the large (~ -17 Hz) $^1J_{NC'}$ couplings.

The expansion of eq 1 to include the proposed factor (eq 2) greatly improved the correlation ($r^2 = 0.861$, Figure 4B):

$$^{h3}J_{NC'(j)} = \{[-1.2\cos^2\alpha_O + (0.41\cos^2\theta_{OC} + 0.15\cos\theta_{OC} - 0.6)\sin^2\alpha_o]\exp[-2.0(d_{HO} - 1.76)]\} \times {}^1/_3[15 + 0.27\sin\psi_{k-1} + 0.9\,{}^1J_\Sigma] \quad (2)$$

where

$$^1J_\Sigma = 0.5\,{}^1J_{NC'(j)} + 0.35\,{}^1J_{NC'(j-1)} + 0.15\,{}^1J_{NC'(j+1)}$$

The correlation between the calculated and experimental $^{h3}J_{NC'}$ values obtained from eq 2 is rather good. However, the deviation of some predicted values is greater than 0.2 Hz, which is larger than the experimental error. We explored whether the incorporation of other parameters that define the complete H-bond geometry of two peptide groups would reduce these deviations. For example, a very weak dependence of $^{h3}J_{NC'}$ on the dihedral angle involving orientation of two peptide-group planes (θ_{HO}) and on the H-bond angle at hydrogen (α_H) has been noted.[4,5] We found that both parameters are significant when introduced into eq 2 by the mechanism of indirect contribution,[4] as sin ($\theta_{HO}/3$) and $\sin^2$ (α_H) terms, respectively. These contributions favor a linear H-bond at a proton site and an antiparallel orientation of the peptide planes. Upon these additions, the $^{h3}J_{NC'}$ couplings calculated using eq 3, have a standard deviation of 0.08 Hz and maximal deviation of 0.16 Hz.

The correlation ($r^2 = 0.884$) between calculated and experimental $^{h3}J_{NC'}$ couplings is presented in Figure 5A. The correlation is successful for all three proteins; the separate correlation coefficients are 0.893 (ubiquitin), 0.835 (holo-CPV), and 0.883 (holo-IFABP):

$$^{h3}J_{NC'(j)} = \{[-1.2\cos^2\alpha_O + [0.7\cos^2\theta_{OC} + 0.55\cos\theta_{OC} - 0.35\sin({}^1/_3\theta_{HO}) - 1.9\sin^2\alpha_H - 0.14]\sin^2\alpha_O]\exp[-2.0(d_{HO} - 1.76)]\} \times [{}^1/_3(15 + 0.27\sin\psi_{k-1} + 0.9\,{}^1J_\Sigma)] \quad (3)$$

where

$$^1J_\Sigma = 0.5\,{}^1J_{NC'(j)} + 0.35\,{}^1J_{NC'(j-1)} + 0.15\,{}^1J_{NC'(j+1)}$$

In Table 2 the contributions to $^{h3}J_{NC'}$ are presented as averages for the secondary structure elements. The coupling constants have the smallest value in reverse turns, and almost double in going from α-helices to β-sheets. The increased couplings are predominantly determined by the H-bond geometry.

H-Bond Networks and $^{h3}J_{NC'}$ Couplings. There are many instances of H-bonds between two peptide groups to which eq 3 is not directly applicable because there is no third peptide group at an "upstream" position. However, the H-bonding at such positions is usually satisfied by polar side chains or water. We cannot account for their individual contributions within a model based on peptide bond $^1J_{NC'(j-1)}$ coupling, but an average effect could be accounted for by ascribing to all of them the standard $^1J_{NC'(j-1)} = -15$ Hz. Using this approximation, all $^{h3}J_{NC'}$ of the proteins' backbone could be interpreted [152 entries: ubiquitin (35), holo-CPV (43), and apo-IFABP (74)], and application of eq 3 gives an r^2 value of 0.77 (Figure 5B). Several points observed as outliers (deviation > 0.2 Hz) suggest exceptional interaction at the "upstream" position. Indeed, two points correspond to the peptide groups from holo-CPV which have their H-bond at the "upstream" position substituted by coordination to Ca^{2+} ion (Figure 6). The sense of deviation is indicative of strong polarizing effects on the peptide bond,[22] as if a strong H-bond is formed at the oxygen site of the peptide

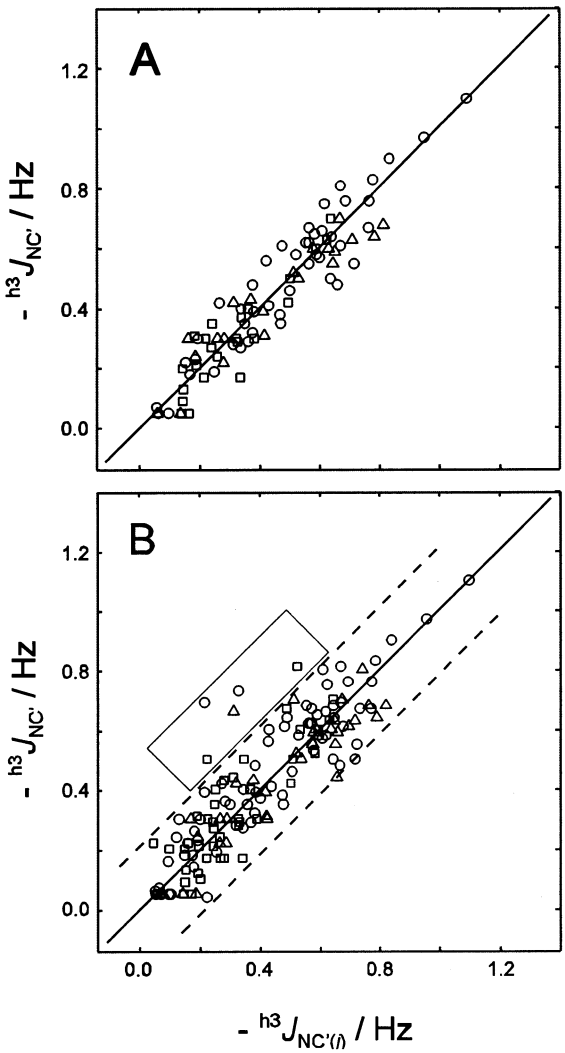

Figure 5. Correlation of $^{h3}J_{NC'}$ couplings with functions of H-bond and peptide bond geometry for human ubiquitin (△), holo-CPV (□), and apo-IFABP (○). (A) Best fit ($r^2 = 0.885$) that requires three peptide groups (91 entries), eq 3. (B) Same equation ($r^2 = 0.782$) applied to larger database (153 entries), which includes all $^{h3}J_{NC'}$ from protein backbone. Notable deviations from the correlation belong to the following H-bonds from the added entries: 15 ⟹ 3 of ubiquitin, 58 ⟹ 97 and 97 ⟹ 58 of holo-CPV, and 68 ⟹ 80 and 94 ⟹ 79 of apo-IFABP.

Table 2. Averages of $-^{h3}J_{NC'}$ in Secondary Structure Elements[a] (Hz)

element	exp	calc	H-bond[b]	peptide bond[c]
β-turns	0.09	0.12	0.36	0.34
α-helices	0.30	0.30	0.63	0.46
β-sheets	0.55	0.55	0.90	0.60

[a] Average values are given in hertz. [b] Contribution from the first factor in eq 3. [c] Contribution from the second factor in eq 3.

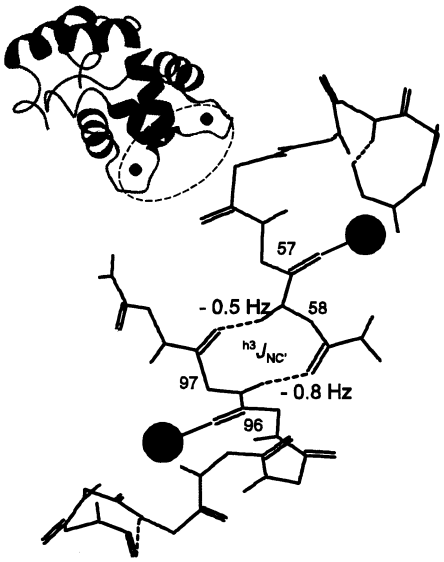

Figure 6. Two H-bonds in the β-sheet motif of holo-CPV (97 ⟹ 58 and 58 ⟹ 97). The oxygen atoms of residues 96 and 57 are coordinated to a calcium ion according to the X-ray crystal structure.[18]

group. Thus, calcium ion ligation affects the H-bonds and the peptide-bonds in the short β-strand that connects the calcium binding sites of holo-CPV. Therefore, it is conceivable that calcium loading at one site changes properties of the other site which could explain the cooperativity of calcium binding to these type of sites.[24] That is, information about loading of one calcium site is transferred to the other via polarization of peptide-bonds and H-bonds between the two sites.

The strong polarization is also expected for peptide groups that are H-bonded by water at the oxygen site.[22,25] In this latter category we identify peptide group 67/68 of apo-IFABP which exhibits the largest deviation in Figure 5B. This is a region of the protein where the presence of a tightly bound water was observed by NMR (negative NOE with amide proton of Val66),[26] and several water molecules are in close proximity to this peptide bond in the crystal structure.[17] Next we identify the peptide group 93/94 of holo-IFABP which also has a H-bond with water according to the crystal structure.

From the ubiquitin data, the peptide group 14/15 is an outlier. This group is at the start of the H-bond chain: 14/15 ⟹ 3/4 ⟹ 65/66, which appears to have an aberrant behavior. Namely, in our study of the correlation between the $^{h3}J_{NC'}$ and $^{1}J_{NC'}$ couplings,[16] the peptide group 3/4 was an outlier which was ascribed to the additional (bifurcated) H-bond from the side chain. Now we see an indication for a strong H-bond at the oxygen site of peptide group 14/15. This oxygen may form contact between an α-helix and β-strand(B) via the side-chain of Lys33 (Figure 7).

Ubiquitin regulates important cellular processes through covalent attachment of the lysine side-chain amino groups.[26] The side-chain of Lys33 is in close proximity to the side-chain of Lys29 which has been identified as the covalent linker.[27]

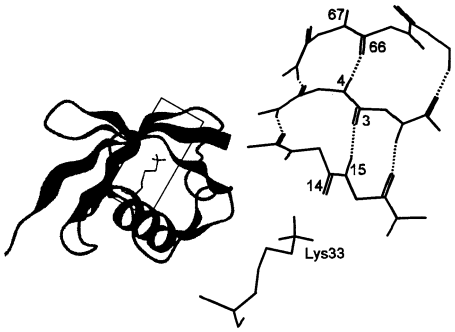

Figure 7. H-bond chain 14/15 ⟹ 3/4 ⟹ 65/66 of ubiquitin in relation to the side chain of Lys33 as seen in the X-ray crystal structure.[17]

The fact that the amino group of Lys33 is available but not used in the covalent linkage may be caused by the H-bond of that group to the carbonyl oxygen of residue 14. The same H-bonding would explain recently observed absence of the interaction between Lys33 and Glu34.[28] In the crystal structure of the metabolically relevant tetraubiquitin,[29] the suggested H-bond of Lys33 is very strong (N···O distance ~ 2.6 Å).

Conclusions

Utilizing the H-bond ($^{h3}J_{NC'}$) and peptide-bond ($^{1}J_{NC'}$) scalar couplings, we have detected chains of H-bonds ranging in length from three to eight peptide groups. We have shown that in these chains $^{h3}J_{NC'}$ is influenced by $^{1}J_{NC'}$ couplings from three peptide groups. Consequently, the structural correlations of $^{h3}J_{NC'}$ couplings in the H-bond chains are also influenced by the structure of peptide groups. By taking these into account, and by using a more complete base of H-bond geometry parameters, we have predicted $^{h3}J_{NC'}$ couplings in the H-bond chains with standard deviations of 0.08 Hz. The functional dependence we have obtained affords observation of some strong disturbances of the H-bond chains: the effect of the calcium ions on the H-bonds in the short β-strand that connects the calcium binding sites of holo-CPV; the aberrant behavior of the H-bond chain in human ubiquitin possibly caused by a strong H-bond of the Lys33 amino group; the polarization of peptide-bond 67/68 of apo-IFABP due to H-bonding of the tightly bound water.

Materials and Methods

Sample Preparations. Uniformly labeled $^{13}C/^{15}N$ human ubiquitin was purchased from VLI Research (Wayne, PA). A sample for NMR measurements (2 mM protein, pH = 4.1) was prepared by dissolving the protein in 25 mM acetic acid-d_4 aqueous solution (5% D_2O). The expression and purification of the $^{13}C/^{15}N$ uniformly labeled parvalbumin mutant (F102W) used in this work has been described previously.[19] The NMR sample (2 mM) was prepared by dissolving lyophilized protein into 0.1 M sodium citrate/sodium acetate (pH 5.6) containing approximately 2 equiv of calcium and 5% D_2O. The expression and purification of the $^{13}C/^{15}N$ uniformly labeled apo-IFABP used in this work has been detailed elsewhere.[30] Purified protein was dialyzed against 20 mM potassium phosphate, pH 5.5, and concentrated to ~1 mM. Sodium azide was added to a final concentration of 0.02%. This solution was further concentrated slowly to 2 mM and 5% D_2O was added for the NMR sample.

(24) Evans, J. S.; Levine, B. A.; Williams, R. J. P.; Wormald, M. R. In *Calmodulin*; Cohen, P., Klee, C. B., Eds.; Elsevier: Amsterdam, 1988; p 68.
(25) Juranić, N.; Likić, A. V.; Prendergast, F. G.; Macura, S. *J. Am. Chem. Soc.* **1996**, *118*, 7859−7860.
(26) Likić, A. V.; Juranić, N.; Macura, S.; Prendergast, F. G. *Protein Sci.* **2000**, *3* 497−504.
(27) Rao, H.; Sastry, A. *J. Biol. Chem.* **2002**, *277*, 1691−1695.
(28) Sundd, M.; Iverson, N.; Ibarra-Molero, B.; Sanchez-Ruiz, J.; Robertson, A. D. *Biochemistry* **2002**, *41*, 7586−7596.
(29) Phillips, C. I.; Thrower, J.; Pickart, C. M.; Hill, C. P. *Acta Crystallogr.* **2001**, *D57*, 341−344.
(30) Kurian, E. Ph.D. Thesis, Mayo Graduate School, Mayo Clinic and Foundation, February 1998, pp 210−212.

NMR Measurements. The H-bond $^{h3}J_{NC'}$ and peptide bond $^{1}J_{NC'}$ coupling constants were measured (Bruker Avance 600 MHz) by a constant time 3D HNCO experiment.[1,2] The constant time was set to ~70 ms for ubiquitin and holo-CPV and to ~35 ms for the faster relaxing apo-IFABP. The experimental $^{n}J_{NC'}$ coupling constants were obtained by fitting the time evolution of all observed NC′ couplings for a particular peptide-group nitrogen (Supporting Information). For each protein, several evolution times were recorded during 6 months (machine time) of measurements. The measurement and determination of the coupling constants were insensitive to their sign; however, they are reported with the negative sign.[3]

H-Bond Geometry Parameters. The angles, dihedral angles, and distances defining the geometry of the H-bond between two peptide groups were calculated from the X-ray structures of three proteins (1ubq.pdb, 4cpv.pdb, and 1ifc.pdb) upon addition of the hydrogens as ridding atoms. The 1ifc.pdb contains two structures (A and B), which were taken with equal weights. The programs for H-bond geometry calculations were written in Matlab (The MathWorks Inc., 1999).

Appendix

Peptide Bond Structure and $^{1}J_{NC'}$ Couplings. The peptide bond is traditionally described as a resonance hybrid of the less polar single-bond and the more polar double-bond structures. Modern high-level quantum-chemical calculations support the validity of this resonance model.[31] One manifestation of the resonance model is the range of peptide bond structures experimentally observed by X-ray analysis. The bonds vary from a single-bond C−N distance in twisted amides to double-bond C═N distance in the imido form of glycylglycine, with a concomitant opposite change in C−O bond order (Figure A1).

Variation of the peptide bond distances in proteins appears to follow the same regularity. However, only in the case of ultrahigh resolution (0.54 Å) structure of a small plant protein, crambin, is the regularity clearly seen. In other high-resolution (<1 Å) protein structures the regularity is statistically significant.[42] The changes of the peptide bond distances in small molecules were found to depend on the hydrogen bonds accepted by the amide oxygen.[43]

The variation of the peptide bond structure is reflected in the change of the $^{1}J_{NC'}$ coupling constant, as presented in Figure A2.

Caution must be exercised when molecules in solution and in crystals are compared. For twisted amides the molecular structures are the same because these molecules are strained and rigid. Acetamide hydrochloride has a protonated amide oxygen (i.e., imino oxygen) in the crystal structure and that molecular structure is preserved when dissolved in trifluoroacetic acid, as evidenced by NMR spectra (Supporting Information). Glycylglycine hydrochloride has regular peptide bond structure in the solid, which was expected to remain unchanged after dissolving in water.

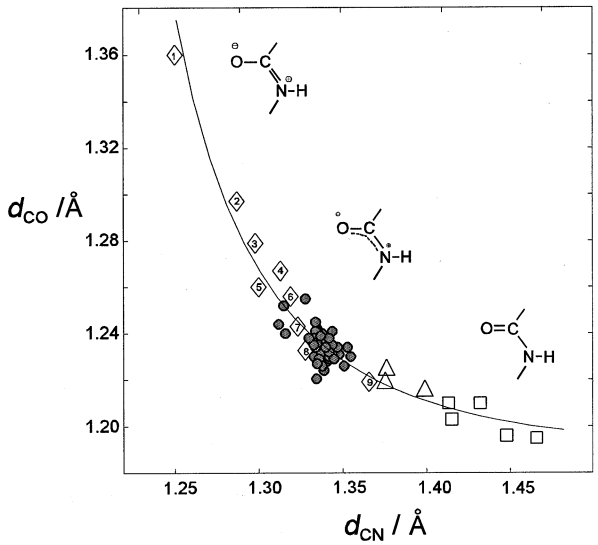

Figure A1. Variations of peptide bond d_{CO} and d_{CN} distances in model compounds [(◇) **1** and **5**, bis(glycylglycinato)cobaltate(III);[32] **2**, acetamide hydrochloride;[33] **3** and **6**, acetamide hydronitrate;[34] **4**, triamine(glycylglycinato)cobalt(III);[35] **7**, *N*-acetylglycine;[36] **8**, glycylglycine hydrochloride;[37] **9**, *N*-methylformamide;[38] (△) bridgehead lactams;[39] (□) twisted amides[40]] and in protein [(●) crambin[41]].

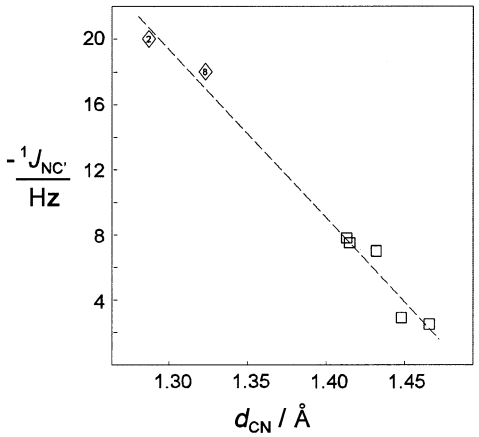

Figure A2. Dependence of $^{1}J_{NC'}$ couplings on CN bond distances in model compounds. Markings and structural references are the same as in Figure 1a. Couplings of twisted amides are from the structural reference. Others couplings are determined here anew (**2**, ^{15}N-acetamide hydrochloride in TFAA; **8**, glycyl-^{15}N-glycine hydrochloride in water) from ^{13}C−^{15}N splitting in carbonyl carbon 1D spectra.

Supporting Information Available: One figure of the 3D HNCO pulse program, one figure of the fitted time evolution of $^{n}J_{NC'}$ coupling constants, one table with $^{h3}J_{NC'}$ and $^{1}J_{NC'}$ coupling constants and H-bond geometry parameters in the three proteins, one table detailing the H-bond chains of four peptide groups, one table of the source experimental data (^{1}H, ^{13}C, and ^{15}N chemical shifts and $^{h3}J_{NC'}$,$^{1}J_{NC'}$, $^{2}J_{NC'}$, and $^{3}J_{NC'}$ coupling constants), and one figure of a 2D HC correlation spectrum of the acetamide -hydrochloride. This information is available free of charge via the Internet at http://pubs.acs.org.

JA0273288

(31) Fogarasi, G.; Szalay, P. *J. Phys. Chem.* **1997**, *101*, 1400−1408.
(32) Barnet, M. T.; Freeman, H. C.; Buckingham, D. A.; Hsu, I.-N.; van der Helm, *Chem. Commun.* **1970**, 367−369.
(33) Liu, L.-K.; Luo, P.-T.; Hsieh, L.-C. *Acta Crystallogr.* **1994**, *C50*, 1333−1335.
(34) Gubin, A. I.; Burnabaev, M. Zh.; Nurakhmetov, N. N. *Kristallografiya* **1988**, *33*, 506−508.
(35) Newman, P. D.; Williams, P. A.; Stephens, F. S.; Vagg, R. S. *Inorg. Chim. Acta* **1991**, *183*, 145−155.
(36) Donohue, J.; Marsh, R. E. *Acta Crystallogr.* **1962**, *15*, 941−945.
(37) Kotzle, T. F.; Hanilton, W. C.; Parthasarathy, R. *Acta Crystallogr.* **1972**, *B28*, 2083−2090.
(38) Kitano, M.; Kuchitsy, K. *Bull. Chem. Soc. Jpn.* **1974**, *47*, 631−639.
(39) Timothy, G. L.; Shea, K. J. *J Am. Chem. Soc.* **1993**, *115*, 2248−2260.
(40) Yamada, S. *J. Org. Chem.* **1996**, *61*, 941−946.
(41) Jelsch, C.; Teeter, M. M.; Lamzin, V.; Pichon-Lesme, V.; Blessing, B.; Lecomte, C. *Proc. Natl. Acad. Sci. U.S.A.* **2000**, *97*, 3171−3176.
(42) Esposito, L.; Vitagliano, L.; Zagari, A.; Mazzarella, L. *Protein Eng.* **2000**, *1*, 825−828.
(43) (a) Popelier, P.; Lenstra, A. T. H.; Van Alenoy, C.; Geise, H. J. *Struct. Chem.* **1990**, *2*, 3−9. (b) Jeffrerey, G. A.; Ruble, R. J.; McMullan, R. K.; DeFrees, D. J.; Binkley, J. S.; Pople, J. A. *Acta Crystallogr.* **1980**, *B36*, 2292−2299.